A Unified Fuzzy Model-Based Framework for Modeling and Control of Complex Systems: From Flying Vehicle Control to Brain-Machine Cooperative Control*

Kazuo Tanaka

Department of Mechanical Engineering and Intelligent Systems,
The University of Electro-Communications,
1-5-1 Chofugaoka, Chofu, Tokyo 182-8585, Japan
ktanaka@mce.uec.ac.jp

Abstract. The invited lecture in 2012 IEEE World Congress on Computational Intelligence (WCCI 2012) presents an overview of a unified fuzzy model-based framework for modeling and control of complex systems. A number of practical applications, ranging from flying vehicles control (including micro helicopter control) to brain-machine cooperative control, are provided in the lecture. The theory and applications have been developed in our laboratory [1] at the University of Electro-Communications (UEC), Tokyo, Japan, in collaboration with Prof. Hua O. Wang and his laboratory [2] at Boston University, Boston, USA. Due to lack of space, this chapter focuses on a unified fuzzy model-based framework for modeling and control of a micro helicopter that is a key application in our research.

1 Introduction

Unmanned aerial vehicles (UAVs) have been an active area of research in recent years. A large number of studies [3] on helicopter control have been conducted as a typical application of UAVs over the last two decades. It is well known that helicopter control is a difficult and challenging problem due to its properties like instability, nonlinearity and coupling, etc. As be mentioned in [3], Sugeno and his group have presented several pioneer and excellent works [4,5] in 1980s and 1990s.

In recent years, in parallel with researches on micro air vehicles (MAVs), autonomous control of micro (small) helicopter (like palm-size helicopters) [6]-[23] has been paid great attention. Due to its restricted payload, the studies [6]-[9] utilize external sensors like CCD camera-type vision sensors. However, use of external vision sensors makes autonomous flight so difficult. The main disadvantage is that micro helicopters can not be controlled in outside vision

* This work has been done in our laboratory [1] at the University of Electro-Communications (UEC), Tokyo, Japan, in collaboration with Prof. Hua O. Wang and his laboratory [2] at Boston University, Boston, USA.

J. Liu et al. (Eds.): WCCI 2012 Plenary/Invited Lectures, LNCS 7311, pp. 185–208, 2012.

sensing area. The study [24] deals with hovering of a micro helicopter carrying vision sensors. However, to accomplish the hovering control, they set up external markers outside the helicopter. As well as the external sensor problem, use of external markers makes autonomous flight so difficult. In addition, the studies [24]-[27] provide no theoretical guarantees of the stability of control system.

Our research targets are to achieve autonomous control of a micro helicopter without any external sensors and markers and to design a controller (theoretically) guaranteeing some kinds of control performance in addition to global and asymptotical stability of control system. The former and latter parts of this chapter focus on the achievement of the second and first targets, respectively.

The pioneer and excellent works by Sugeno and co-workers [4,5] applied traditional model-free fuzzy control to a (large-size) RC helicopter. The author [6] also applied model-free fuzzy control to a micro (palm-size) helicopter. Though the works [4,5] by Sugeno and co-workers particularly achieve great flight control performance such as hovering, turning, taking off and landing by using fuzzy control rules obtained from expert's knowledge and operation manuals, the model-free approaches provide no theoretical guarantees of the stability of control system. In this chapter, to guarantee some kinds of control performance in addition to global and asymptotical stability, we apply two innovative fuzzy model-based control approaches to a micro helicopter. One is a linear matrix inequality (LMI) approach [28] that is a well-known approach and has been widely used in control system design and analysis over the last decade. The other is a sum of squares (SOS) approach [29]-[33] recently presented by the author and co-workers. These [29]-[33] are completely different approaches from the existing LMI approaches. To the best of our knowledge, the paper [29] presented the first attempt at applying an SOS to fuzzy systems. Our SOS approach [29]-[33] provided more extensive results for the existing LMI approaches to Takagi-Sugeno fuzzy model and control. SOS design conditions can be symbolically and numerically solved via the SOSTOOLS [34] and the SeDuMi[35].

Section 2 presents our experimental system and micro helicopter dynamics. In Section 3, we summarize a recent developed SOS design approach for polynomial fuzzy control systems based on polynomial Lyapunov functions. Due to lack of space, we will omit the explanation of LMI-based design approach to Takagi-Sugeno fuzzy systems. For more details of the approach, see [28]. In Section 4, we present a comparison result of a micro helicopter via the LMI and SOS approaches. The simulation result shows that the SOS approach provides better results than the existing LMI approach. Finally, in Section 5, we apply one of the control approaches discussed here to vision-based control of the micro helicopter in real environments [36].

2 Micro Helicopter Dynamics

Fig. 2 shows the micro helicopter that we consider in this study. The helicopter with coaxial counter-rotating blades has two features. One is that rotating torque of yaw-direction of the main body can be canceled by rotating torques between

the upper and lower rotors. In other words, the body-turn can be achieved by generating a difference of rotating torques between the upper and lower rotors. The other is that a mechanical stabilizer attached above the upper rotor has a function of keeping the upper rotor horizontally. The two features will be considered in the dynamic model construction. The dynamics of the helicopter can be described as (1)-(6).

$$m(\dot{u}(t) + q(t)w(t) - r(t)v(t)) = F_X(t) \tag{1}$$
$$m(\dot{v}(t) + r(t)u(t) - p(t)w(t)) = F_Y(t) \tag{2}$$
$$m(\dot{w}(t) + p(t)v(t) - q(t)u(t)) = F_Z(t) \tag{3}$$
$$\dot{p}(t)I_X + q(t)r(t)(I_Z - I_Y) = M_X(t) \tag{4}$$
$$\dot{q}(t)I_Y + r(t)p(t)(I_X - I_Z) = M_Y(t) \tag{5}$$
$$\dot{r}(t)I_Z + p(t)q(t)(I_Y - I_X) = M_Z(t) \tag{6}$$

Table 1 shows the definition of variables used in the dynamic models. By considering its co-axial counter structure, the restitutive force (generated by a mechanical stabilizer attached on the helicopter) and gravity compensation, the dynamics can be rewritten as

$$\dot{u}(t) = r(t)v(t) + \frac{1}{m}U_X(t), \tag{7}$$
$$\dot{v}(t) = -r(t)u(t) + \frac{1}{m}U_Y(t), \tag{8}$$
$$\dot{w}(t) = \frac{1}{m}U_Z(t), \tag{9}$$
$$\dot{\psi}(t) = \frac{1}{I_Z}U_\psi(t), \tag{10}$$

Table 1. Definition of variables

x, u	position and velocity (X-axis)
y, v	position and velocity (Y-axis)
z, w	position and velocity (Z-axis)
ϕ, p	angle and angle velocity (X-axis)
θ, q	angle and angle velocity (Y-axis)
ψ, r	angle and angle velocity (Z-axis)
m	mass
I_X, I_Y, I_Z	moments of inertia with respect to X, Y and Z axes
F_X, F_Y, F_Z	translational forces to X, Y and Z axes
M_X, M_Y, M_Z	rotational forces around X, Y and Z axes

where $m = 0.2$ and $I_z = 0.2857$. $U_X(t)$, $U_Y(t)$, $U_Z(t)$ and $U_\psi(t)$ denote new control input variables. We can obtain the original control inputs (to the real helicopter) from $U_X(t)$, $U_Y(t)$, $U_Z(t)$ and $U_\psi(t)$.

3 Polynomial Fuzzy Model and SOS-Based Designs

In general, LMI conditions can be solved numerically and efficiently by interior point algorithms, e.g., by the Robust Control Toolbox of MATLAB[1]. On the other hand, stability [29], stabilization conditions [30,31], guaranteed cost control [32,33] for polynomial fuzzy systems and polynomial Lyapunov functions reduce to SOS problems. Clearly, the problem is never solved by LMI solvers and can be solved via the SOSTOOLS [34] and the SeDuMi[35].

SOSTOOLS [34] is a free, third party MATLAB toolbox for solving sum of squares problems. The techniques behind it are based on the sum of squares decomposition for multivariate polynomials, which can be efficiently computed using semidefinite programming. SOSTOOLS is developed as a consequence of the recent interest in sum of squares polynomials, partly due to the fact that these techniques provide convex relaxations for many hard problems such as global, constrained, and boolean optimization. For more details, see the manual of SOSTOOLS [34].

3.1 Polynomial Fuzzy Model and Controller

In [29], we proposed a new type of fuzzy model with polynomial model consequence, i.e., fuzzy model whose consequent parts are represented by polynomials. Consider the following nonlinear system:

$$\dot{\boldsymbol{x}}(t) = \boldsymbol{f}(\boldsymbol{x}(t), \boldsymbol{u}(t)), \tag{11}$$

where $\boldsymbol{f}$ is a nonlinear function. $\boldsymbol{x}(t) = [x_1(t)\ x_2(t)\ \cdots\ x_n(t)]^T$ is the state vector and $\boldsymbol{u}(t) = [u_1(t)\ u_2(t)\ \cdots\ u_m(t)]^T$ is the input vector. Using the sector nonlinearity concept [28], we exactly represent (11) with the following polynomial fuzzy model (12). The main difference between the Takagi-Sugeno fuzzy model [37] and the polynomial fuzzy model (12) is consequent part representation. The fuzzy model (12) has a polynomial model consequence.

Model Rule i**:**

$$\begin{aligned} &If\ z_1(t)\ is\ M_{i1}\ and \cdots\ and\ \ z_p(t)\ is\ M_{ip} \\ &then\ \dot{\boldsymbol{x}}(t) = \boldsymbol{A}_i(\boldsymbol{x}(t))\hat{\boldsymbol{x}}(\boldsymbol{x}(t)) + \boldsymbol{B}_i(\boldsymbol{x}(t))\boldsymbol{u}(t), \end{aligned} \tag{12}$$

where $i = 1, 2, \cdots, r$. r denotes the number of $Model\ Rules$. $z_j(t)$ $(j = 1, 2, \cdots, p)$ is the premise variable. The membership function associated with the ith $Model\ Rule$ and jth premise variable component is denoted by M_{ij}. Each $z_j(t)$ is a measurable time-varying quantity that may be states, measurable external variables and/or time. $\boldsymbol{A}_i(\boldsymbol{x}(t))$ and $\boldsymbol{B}_i(\boldsymbol{x}(t))$ are polynomial matrices in $\boldsymbol{x}(t)$. $\hat{\boldsymbol{x}}(\boldsymbol{x}(t))$ is a column vector whose entries are all monomials in $\boldsymbol{x}(t)$. That is, $\hat{\boldsymbol{x}}(\boldsymbol{x}(t)) \in \boldsymbol{R}^N$ is an $N \times 1$ vector of monomials in $\boldsymbol{x}(t)$. Therefore, $\boldsymbol{A}_i(\boldsymbol{x}(t))\hat{\boldsymbol{x}}(\boldsymbol{x}(t))$ $+ \boldsymbol{B}_i(\boldsymbol{x}(t))\boldsymbol{u}(t)$ is a polynomial vector. Thus, the polynomial fuzzy model (12)

[1] A registered trademark of MathWorks, Inc.

has a polynomial in each consequent part. The details of $\hat{\boldsymbol{x}}(\boldsymbol{x}(t))$ will be given in Proposition 1. We assume that

$$\hat{\boldsymbol{x}}(\boldsymbol{x}(t)) = 0 \text{ iff } \boldsymbol{x}(t) = 0$$

throughout this chapter.

The computational method used in this chapter relies on the sum of squares decomposition of multivariate polynomials. A multivariate polynomial $f(\boldsymbol{x}(t))$ (where $\boldsymbol{x}(t) \in R^n$) is a sum of squares (SOS) if there exist polynomials $f_1(\boldsymbol{x}(t))$, $\cdots$, $f_m(\boldsymbol{x}(t))$ such that $f(\boldsymbol{x}(t)) = \sum_{i=1}^{m} f_i^2(\boldsymbol{x}(t))$. It is clear that $f(\boldsymbol{x}(t))$ being an SOS naturally implies $f(\boldsymbol{x}(t)) > 0$ for all $\boldsymbol{x}(t) \in R^n$. This can be shown equivalent to the existence of a special quadric form stated in the following proposition.

Proposition 1. *[38] Let $f(\boldsymbol{x}(t))$ be a polynomial in $\boldsymbol{x}(t) \in R^n$ of degree $2d$. In addition, let $\hat{\boldsymbol{x}}(\boldsymbol{x}(t))$ be a column vector whose entries are all monomials in $\boldsymbol{x}(t)$ with degree no greater than d. Then $f(\boldsymbol{x}(t))$ is a sum of squares iff there exists a positive semidefinite matrix $\boldsymbol{P}$ such that*

$$f(\boldsymbol{x}(t)) = \hat{\boldsymbol{x}}^T(\boldsymbol{x}(t))\boldsymbol{P}\hat{\boldsymbol{x}}(\boldsymbol{x}(t)). \tag{13}$$

Expressing an SOS polynomial using a quadratic form as in (13) has also been referred to as the Gram matrix method.

A monomial in $\boldsymbol{x}(t)$ is a function of the form $x_1^{\alpha_1} x_2^{\alpha_2} \cdots x_n^{\alpha_n}$, where α_1, α_2, $\cdots$, α_n are nonnegative integers. In this case, the degree of the monomial is given by $\alpha_1 + \alpha_1 + \cdots + \alpha_n$.

The defuzzification process of the model (12) can be represented as

$$\dot{\boldsymbol{x}}(t) = \sum_{i=1}^{r} h_i(\boldsymbol{z}(t))\{\boldsymbol{A}_i(\boldsymbol{x}(t))\hat{\boldsymbol{x}}(\boldsymbol{x}(t)) + \boldsymbol{B}_i(\boldsymbol{x}(t))\boldsymbol{u}(t)\}, \tag{14}$$

where

$$h_i(\boldsymbol{z}(t)) = \frac{\prod_{j=1}^{p} M_{ij}(z_j(t))}{\sum_{k=1}^{r} \prod_{j=1}^{p} M_{kj}(z_j(t))}.$$

It should be noted from the properties of membership functions that $h_i(\boldsymbol{z}(t)) \geq 0$ for all i and $\sum_{i=1}^{r} h_i(\boldsymbol{z}(t)) = 1$. Thus, the overall fuzzy model is achieved by fuzzy blending of the polynomial system models. As shown in [29]-[31], the number of rules in polynomial fuzzy model generally becomes fewer than that in T-S fuzzy model, and our SOS approach to polynomial fuzzy models provides much more relaxed stability and stabilization results than the existing LMI approaches to T-S fuzzy model and control.

Since the parallel distributed compensation (PDC) [28] mirrors the structure of the fuzzy model of a system, a fuzzy controller with polynomial rule consequence can be constructed from the given polynomial fuzzy model (12).

Control Rule i:

$$\begin{aligned} &If\ z_1(t)\ is\ M_{i1}\ and \cdots\ and\ \ z_p(t)\ is\ M_{ip} \\ &then\ \boldsymbol{u}(t) = -\boldsymbol{F}_i(\boldsymbol{x}(t))\hat{\boldsymbol{x}}(\boldsymbol{x}(t)) \quad i = 1, 2, \cdots, r \end{aligned} \tag{15}$$

The overall fuzzy controller can be calculated by

$$\boldsymbol{u}(t) = -\sum_{i=1}^{r} h_i(\boldsymbol{z}(t))\boldsymbol{F}_i(\boldsymbol{x}(t))\hat{\boldsymbol{x}}(\boldsymbol{x}(t)). \tag{16}$$

From (14) and (16), the closed-loop system can be represented as

$$\begin{aligned} \dot{\boldsymbol{x}}(t) = &\sum_{i=1}^{r}\sum_{j=1}^{r} h_i(\boldsymbol{z}(t))h_j(\boldsymbol{z}(t)) \\ &\times \{\boldsymbol{A}_i(\boldsymbol{x}(t)) - \boldsymbol{B}_i(\boldsymbol{x}(t))\boldsymbol{F}_j(\boldsymbol{x}(t))\}\hat{\boldsymbol{x}}(\boldsymbol{x}(t)). \end{aligned} \tag{17}$$

If $\hat{\boldsymbol{x}}(\boldsymbol{x}(t)) = \boldsymbol{x}(t)$ and $\boldsymbol{A}_i(\boldsymbol{x}(t))$, $\boldsymbol{B}_i(\boldsymbol{x}(t))$ and $\boldsymbol{F}_j(\boldsymbol{x}(t))$ are constant matrices for all i and j, then (14) and (16) reduce to the Takagi-Sugeno fuzzy model and controller, respectively. Therefore, (14) and (16) are more general representation.

3.2 Stable Control

To obtain more relaxed stability results, we employ a polynomial Lyapunov function [29] represented by

$$\hat{\boldsymbol{x}}^T(\boldsymbol{x}(t))\boldsymbol{P}(\tilde{\boldsymbol{x}}(t))\hat{\boldsymbol{x}}(\boldsymbol{x}(t)), \tag{18}$$

where $\boldsymbol{P}(\tilde{\boldsymbol{x}}(t))$ is a polynomial matrix in $\boldsymbol{x}(t)$. If $\hat{\boldsymbol{x}}(t) = \boldsymbol{x}(t)$ and $\boldsymbol{P}(\tilde{\boldsymbol{x}}(t))$ is a constant matrix, then (18) reduces to the quadratic Lyapunov function $\boldsymbol{x}^T(t)\boldsymbol{P}\boldsymbol{x}(t)$. Therefore, (18) is a more general representation.

From now, to lighten the notation, we will drop the notation with respect to time t. For instance, we will employ $\boldsymbol{x}$, $\hat{\boldsymbol{x}}(\boldsymbol{x})$ instead of $\boldsymbol{x}(t)$, $\hat{\boldsymbol{x}}(\boldsymbol{x}(t))$, respectively. Thus, we drop the notation with respect to time t, but it should be kept in mind that $\boldsymbol{x}$ means $\boldsymbol{x}(t)$.

Let $\boldsymbol{A}_i^k(\boldsymbol{x})$ denotes the k-th row of $\boldsymbol{A}_i(\boldsymbol{x})$, $\boldsymbol{K} = \{k_1, k_2, \cdots k_m\}$ denote the row indices of $\boldsymbol{B}_i(\boldsymbol{x})$ whose corresponding row is equal to zero, and define $\tilde{\boldsymbol{x}} = (x_{k_1}, x_{k_2}, \cdots x_{k_m})$.

Theorem 1. *[30] The control system consisting of (14) and (16) is stable if there exist a symmetric polynomial matrix $\boldsymbol{X}(\tilde{\boldsymbol{x}}) \in \boldsymbol{R}^{N\times N}$ and a polynomial matrix $\boldsymbol{M}_i(\boldsymbol{x}) \in \boldsymbol{R}^{m\times N}$ such that (19) and (20) are satisfied, where $\epsilon_1(\boldsymbol{x})$ and $\epsilon_{2ij}(\boldsymbol{x})$ are non negative polynomials such that $\epsilon_1(\boldsymbol{x}) > 0$ $(\boldsymbol{x} \neq 0)$ and $\epsilon_{2ij}(\boldsymbol{x}) \geq 0$ for all $\boldsymbol{x}$.*

$$\boldsymbol{v}^T(\boldsymbol{X}(\tilde{\boldsymbol{x}}) - \epsilon_1(\boldsymbol{x})\boldsymbol{I})\boldsymbol{v} \; is \; SOS \tag{19}$$

$$\begin{aligned}
&-\boldsymbol{v}^T \big(\boldsymbol{T}(\boldsymbol{x})\boldsymbol{A}_i(\boldsymbol{x})\boldsymbol{X}(\tilde{\boldsymbol{x}}) - \boldsymbol{T}(\boldsymbol{x})\boldsymbol{B}_i(\boldsymbol{x})\boldsymbol{M}_j(\boldsymbol{x}) \\
&\quad + \boldsymbol{X}(\tilde{\boldsymbol{x}})\boldsymbol{A}_i^T(\boldsymbol{x})\boldsymbol{T}^T(\boldsymbol{x}) - \boldsymbol{M}_j^T(\boldsymbol{x})\boldsymbol{B}_i^T(\boldsymbol{x})\boldsymbol{T}^T(\boldsymbol{x}) \\
&\quad + \boldsymbol{T}(\boldsymbol{x})\boldsymbol{A}_j(\boldsymbol{x})\boldsymbol{X}(\tilde{\boldsymbol{x}}) - \boldsymbol{T}(\boldsymbol{x})\boldsymbol{B}_j(\boldsymbol{x})\boldsymbol{M}_i(\boldsymbol{x}) \\
&\quad + \boldsymbol{X}(\tilde{\boldsymbol{x}})\boldsymbol{A}_j^T(\boldsymbol{x})\boldsymbol{T}^T(\boldsymbol{x}) - \boldsymbol{M}_i^T(\boldsymbol{x})\boldsymbol{B}_j^T(\boldsymbol{x})\boldsymbol{T}^T(\boldsymbol{x}) \\
&\quad - \sum_{k\in\boldsymbol{K}} \frac{\partial \boldsymbol{X}}{\partial x_k}(\tilde{\boldsymbol{x}})\boldsymbol{A}_i^k(\boldsymbol{x})\hat{\boldsymbol{x}}(\boldsymbol{x}) \\
&\quad - \sum_{k\in\boldsymbol{K}} \frac{\partial \boldsymbol{X}}{\partial x_k}(\tilde{\boldsymbol{x}})\boldsymbol{A}_j^k(\boldsymbol{x})\hat{\boldsymbol{x}}(\boldsymbol{x}) + \epsilon_{2ij}(\boldsymbol{x})\boldsymbol{I}\Big)\boldsymbol{v} \; is \; SOS \quad i \le j,
\end{aligned} \tag{20}$$

where $\boldsymbol{v} \in R^N$ is a vector that is independent of $\boldsymbol{x}$. $\boldsymbol{T}(\boldsymbol{x}) \in \boldsymbol{R}^{N\times n}$ is a polynomial matrix whose (i, j)-th entry is given by $T^{ij}(\boldsymbol{x}) = \frac{\partial \hat{x}_i}{\partial x_j}(\boldsymbol{x})$. In addition, if (20) holds with $\epsilon_{2ij}(\boldsymbol{x}) > 0$ for $\boldsymbol{x} \neq 0$, then the zero equilibrium is asymptotically stable. If $\boldsymbol{X}(\tilde{\boldsymbol{x}})$ is a constant matrix, then the stability holds globally. A stabilizing feedback gain $\boldsymbol{F}_i(\boldsymbol{x})$ can be obtained from $\boldsymbol{X}(\tilde{\boldsymbol{x}})$ and $\boldsymbol{M}_i(\boldsymbol{x})$ as $\boldsymbol{F}_i(\boldsymbol{x}) = \boldsymbol{M}_i(\boldsymbol{x})\boldsymbol{X}^{-1}(\tilde{\boldsymbol{x}})$.

3.3 Guaranteed Cost Control

For the polynomial fuzzy model (14) and controller (16), we define the polynomial fuzzy model output as

$$\boldsymbol{y} = \sum_{i=1}^{r} h_i(\boldsymbol{z})\boldsymbol{C}_i(\boldsymbol{x})\hat{\boldsymbol{x}}(\boldsymbol{x}), \tag{21}$$

where $\boldsymbol{C}_i(\boldsymbol{x})$ is also a polynomial matrix. Let us consider the following performance function to be optimized.

$$J = \int_0^\infty \hat{\boldsymbol{y}}^T \begin{bmatrix} \boldsymbol{Q} & \boldsymbol{0} \\ \boldsymbol{0} & \boldsymbol{R} \end{bmatrix} \hat{\boldsymbol{y}} dt, \tag{22}$$

where

$$\hat{\boldsymbol{y}} = \begin{bmatrix} \boldsymbol{y} \\ \boldsymbol{u} \end{bmatrix} = \sum_{i=1}^{r}\sum_{j=1}^{r} h_i(\boldsymbol{z})h_j(\boldsymbol{z}) \begin{bmatrix} \boldsymbol{C}_i(\boldsymbol{x}) \\ -\boldsymbol{F}_j(\boldsymbol{x}) \end{bmatrix} \hat{\boldsymbol{x}}(\boldsymbol{x}), \tag{23}$$

$\boldsymbol{Q}$ and $\boldsymbol{R}$ are positive definite matrices.

Theorem 2 provides the SOS design condition that minimizes the upper bound of the given performance function (22).

Theorem 2. *[32] If there exist a symmetric polynomial matrix $\boldsymbol{X}(\tilde{\boldsymbol{x}}) \in \boldsymbol{R}^{N\times N}$ and a polynomial matrix $\boldsymbol{M}_i(\boldsymbol{x}) \in \boldsymbol{R}^{m\times N}$ such that (24), (25), (26) and (27) hold, the guaranteed cost controller that minimizes the upper bound of the given performance function (22) can be designed as $\boldsymbol{F}_i(\boldsymbol{x}) = \boldsymbol{M}_i(\boldsymbol{x})\boldsymbol{X}^{-1}(\tilde{\boldsymbol{x}})$.*

$$
\begin{aligned}
&\underset{X(\tilde{\boldsymbol{x}}),M_i(\boldsymbol{x})}{minimize} \qquad \lambda \\
&subject\ to \\
&\boldsymbol{v}_1^T(\boldsymbol{X}(\tilde{\boldsymbol{x}}) - \epsilon_1(\boldsymbol{x})\boldsymbol{I})\boldsymbol{v}_1 \ is\ SOS \qquad (24)\\
&\boldsymbol{v}_2^T \begin{bmatrix} \lambda & \hat{\boldsymbol{x}}^T(\boldsymbol{0}) \\ \hat{\boldsymbol{x}}(\boldsymbol{0}) & \boldsymbol{X}(\tilde{\boldsymbol{x}}(\boldsymbol{0})) \end{bmatrix} \boldsymbol{v}_2 \ is\ SOS \qquad (25)\\
&-\boldsymbol{v}_3^T \begin{bmatrix} \boldsymbol{N}_{ii}(\boldsymbol{x}) + \epsilon_{2ii}(\boldsymbol{x})\boldsymbol{I} & * & * \\ \boldsymbol{C}_i(\boldsymbol{x})\boldsymbol{X}(\tilde{\boldsymbol{x}}) & -\boldsymbol{Q}^{-1} & * \\ -\boldsymbol{M}_i(\boldsymbol{x}) & \boldsymbol{0} & -\boldsymbol{R}^{-1} \end{bmatrix} \boldsymbol{v}_3 \ is\ SOS, \qquad (26)\\
&-\boldsymbol{v}_4^T \begin{bmatrix} \boldsymbol{N}_{ij}(\boldsymbol{x}) + \boldsymbol{N}_{ji}(\boldsymbol{x}) & * & * \\ \begin{pmatrix} \boldsymbol{C}_i(\boldsymbol{x})\boldsymbol{X}(\tilde{\boldsymbol{x}}) \\ +\boldsymbol{C}_j(\boldsymbol{x})\boldsymbol{X}(\tilde{\boldsymbol{x}}) \end{pmatrix} & -2\boldsymbol{Q}^{-1} & \boldsymbol{0} \\ -\boldsymbol{M}_i(\boldsymbol{x}) - \boldsymbol{M}_j(\boldsymbol{x}) & \boldsymbol{0} & -2\boldsymbol{R}^{-1} \end{bmatrix} \boldsymbol{v}_4 \ is\ SOS, \quad i<j, \qquad (27)
\end{aligned}
$$

*where * denotes the transposed elements (matrices) for symmetric positions.*

$$
\begin{aligned}
\boldsymbol{N}_{ij}(\boldsymbol{x}) =& \boldsymbol{T}(\boldsymbol{x})\boldsymbol{A}_i(\boldsymbol{x})\boldsymbol{X}(\tilde{\boldsymbol{x}}) - \boldsymbol{T}(\boldsymbol{x})\boldsymbol{B}_i(\boldsymbol{x})\boldsymbol{M}_j(\boldsymbol{x}) \\
&+ \boldsymbol{X}(\tilde{\boldsymbol{x}})\boldsymbol{A}_i^T(\boldsymbol{x})\boldsymbol{T}^T(\boldsymbol{x}) - \boldsymbol{M}_j^T(\boldsymbol{x})\boldsymbol{B}_i^T(\boldsymbol{x})\boldsymbol{T}^T(\boldsymbol{x}) \\
&- \sum_{k\in\boldsymbol{K}} \frac{\partial \boldsymbol{X}(\tilde{\boldsymbol{x}})}{\partial x_k}\boldsymbol{A}_i^k(\boldsymbol{x})\hat{\boldsymbol{x}}.
\end{aligned}
$$

$\boldsymbol{v}_1$, $\boldsymbol{v}_2$, $\boldsymbol{v}_3$ and $\boldsymbol{v}_4$ are vectors that are independent of $\boldsymbol{x}$. $\epsilon_1(\boldsymbol{x})$ and $\epsilon_{2ii}(\boldsymbol{x})$ are non negative polynomials such that $\epsilon_1(\boldsymbol{x}) > 0$ and $\epsilon_{2ii}(\boldsymbol{x}) > 0$ at $\boldsymbol{x} \neq \boldsymbol{0}$, and $\epsilon_1(\boldsymbol{x}) = 0$ and $\epsilon_{2ii}(\boldsymbol{x}) = 0$ at $\boldsymbol{x} = \boldsymbol{0}$.

Remark 1. *Note that $\boldsymbol{v}_1$, $\boldsymbol{v}_2$, $\boldsymbol{v}_3$ and $\boldsymbol{v}_4$ are vectors that are independent of $\boldsymbol{x}$, because $\boldsymbol{L}(\boldsymbol{x})$ is not always a positive semi-definite matrix for all $\boldsymbol{x}$ even if $\boldsymbol{x}^T(\boldsymbol{x})\boldsymbol{L}(\boldsymbol{x})\boldsymbol{x}(\boldsymbol{x})$ is an SOS, where $\boldsymbol{L}(\boldsymbol{x})$ is a symmetric polynomial matrix in $\boldsymbol{x}(t)$. However, it is guaranteed from Proposition 2 in [32] that if $\boldsymbol{v}^T\boldsymbol{L}(\boldsymbol{x})\boldsymbol{v}$ is an SOS, then $\boldsymbol{L}(\boldsymbol{x}) \geq 0$ for all $\boldsymbol{x}$.*

Remark 2. *To avoid introducing non-convex condition, we assume that $\boldsymbol{X}(\tilde{\boldsymbol{x}})$ only depends on states $\tilde{\boldsymbol{x}}$ whose dynamics is not directly affected by the control input, namely states whose corresponding rows in $\boldsymbol{B}_i(\boldsymbol{x})$ are zero. In relation to this, it may be advantageous to employ an initial state transformation to introduce as many zero rows as possible in $\boldsymbol{B}_i(\boldsymbol{x})$.*

Remark 3. *When $\boldsymbol{X}(\tilde{\boldsymbol{x}})$ is a constant matrix and $\hat{\boldsymbol{x}}(\boldsymbol{x}) = \boldsymbol{x}$, the system representation is the same as the Takagi-Sugeno fuzzy model and control used in many of the references, e.g., [28,39]. Thus, our SOS approach to fuzzy model and control with polynomial rule consequence contains the existing LMI approaches to Takagi-Sugeno fuzzy model and control as a special case. Therefore, our SOS approach provides much more relaxed results than the existing approaches to Takagi-Sugeno fuzzy model and control.*

4 Controller Designs

For the dynamics of the helicopter (7)-(10), we consider the local linear feedback control with respect to the yaw angle $\psi(t)$. From the practical control points of view, we design a local stable feedback controller $U_\psi(t) = -a \cdot \psi(t)$, where a is a positive value. Clearly, the yaw dynamics can be stabilized by the local feedback controller. As a result, we can focus on the remaining $x(t)$, $y(t)$ and $z(t)$ position control. Then, the dynamics can be rewritten as

$$\dot{u}(t) = -\frac{a}{I_z}\psi(t)v(t) + \frac{1}{m}U_X(t), \tag{28}$$

$$\dot{v}(t) = \frac{a}{I_z}\psi(t)u(t) + \frac{1}{m}U_Y(t), \tag{29}$$

$$\dot{w}(t) = \frac{1}{m}U_Z(t). \tag{30}$$

Based on the concept of sector nonlinearity [28], the nonlinear system can be exactly represented by a Takagi-Sugeno fuzzy model for $\psi(t) \in [-\pi\ \pi]$. The Takagi-Sugeno fuzzy model is obtained as

$$\dot{\boldsymbol{x}}(t) = \sum_{i=1}^{2} h_i(\boldsymbol{z}(t))\{\boldsymbol{A}_i\boldsymbol{x}(t) + \boldsymbol{B}_i\boldsymbol{u}(t)\}, \tag{31}$$

$$\dot{\boldsymbol{y}}(t) = \sum_{i=1}^{2} h_i(\boldsymbol{z}(t))\boldsymbol{C}_i\boldsymbol{x}(t), \tag{32}$$

where $\boldsymbol{z}(t) = \psi(t)$ and

$$\boldsymbol{x}(t) = [u(t)\ v(t)\ w(t)\ e_x(t)\ e_y(t)\ e_z(t)]^T,$$
$$\boldsymbol{u}(t) = [U_X(t)\ U_Y(t)\ U_Z(t)]^T.$$

The elements $e_x(t), e_y(t)$ and $e_z(t)$ are defined as $e_x(t) = x(t) - x_{ref}, e_y(t) = y(t) - y_{ref}, e_z(t) = z(t) - z_{ref}$, where x_{ref}, y_{ref} and z_{ref} are constant target positions. $\boldsymbol{A}_i$, $\boldsymbol{B}_i$ and $\boldsymbol{C}_i$ matrices and the membership functions are given as follows.

$$\boldsymbol{A}_1 = \begin{bmatrix} 0 & -\frac{a\pi}{I_Z} & 0 & 0 & 0 & 0 \\ \frac{a\pi}{I_Z} & 0 & 0 & 0 & 0 & 0 \\ 0 & 0 & 0 & 0 & 0 & 0 \\ 1 & 0 & 0 & 0 & 0 & 0 \\ 0 & 1 & 0 & 0 & 0 & 0 \\ 0 & 0 & 1 & 0 & 0 & 0 \end{bmatrix}, \quad \boldsymbol{A}_2 = \begin{bmatrix} 0 & \frac{a\pi}{I_Z} & 0 & 0 & 0 & 0 \\ -\frac{a\pi}{I_Z} & 0 & 0 & 0 & 0 & 0 \\ 0 & 0 & 0 & 0 & 0 & 0 \\ 1 & 0 & 0 & 0 & 0 & 0 \\ 0 & 1 & 0 & 0 & 0 & 0 \\ 0 & 0 & 1 & 0 & 0 & 0 \end{bmatrix},$$

$$\boldsymbol{B}_1 = \boldsymbol{B}_2 = \begin{bmatrix} \frac{1}{m} & 0 & 0 \\ 0 & \frac{1}{m} & 0 \\ 0 & 0 & \frac{1}{m} \\ 0 & 0 & 0 \\ 0 & 0 & 0 \\ 0 & 0 & 0 \end{bmatrix}, \quad \boldsymbol{C}_1 = \boldsymbol{C}_2 = \begin{bmatrix} 0\,0\,0\,1\,0\,0 \\ 0\,0\,0\,0\,1\,0 \\ 0\,0\,0\,0\,0\,1 \end{bmatrix},$$

$$h_1(\psi(t)) = \frac{\psi(t)+\pi}{2\pi}\ ,\ h_2(\psi(t)) = \frac{\pi-\psi(t)}{2\pi}.$$

Note that the Takagi-Sugeno fuzzy model exactly represents the dynamics (28) - (30) for the range $\psi(t) \in [-\pi\ \pi]$. In addition, the local stable controller $U_\psi(t) = -a \cdot \psi(t)$ guarantees $\psi(t_1) > \psi(t_2)$ for $t_1 < t_2$. The asymptotic stability property means that the helicopter describing by the dynamics (7) - (10) can be stabilized if we can design a stable controller for (28) - (30).

4.1 LMI Design Approach

Consider the performance index (22) again. We can find feedback gains that minimizes the upper bound of (22) by solving the following LMIs [28]. From the solutions $\boldsymbol{X}$ and $\boldsymbol{M_i}$, the feedback gains can be obtained as $\boldsymbol{F}_i = \boldsymbol{M}_i\boldsymbol{X}^{-1}$. Then, the controller satisfies $J < \boldsymbol{x}^T(0)\boldsymbol{X}\boldsymbol{x}(0) < \lambda$.

$$\begin{aligned} &\underset{\boldsymbol{X},\boldsymbol{M_i},}{minimize}\ \lambda \\ &subject\ \ to \end{aligned}$$

$$\boldsymbol{X} > \boldsymbol{0},\ \begin{bmatrix} \lambda & \boldsymbol{x}^T(0) \\ \boldsymbol{x}(0) & \boldsymbol{X} \end{bmatrix} > \boldsymbol{0}, \tag{33}$$

$$\hat{\boldsymbol{U}}_{ii} < \boldsymbol{0} \tag{34}$$

$$\hat{\boldsymbol{V}}_{ij} < \boldsymbol{0} \qquad i < j, \tag{35}$$

where

$$\hat{\boldsymbol{U}}_{ii} = \begin{bmatrix} \boldsymbol{H}_{ii} & \boldsymbol{X}\boldsymbol{C}_i^T & -\boldsymbol{M}_i^T \\ \boldsymbol{C}_i\boldsymbol{X} & -\boldsymbol{Q}^{-1} & \boldsymbol{0} \\ -\boldsymbol{M}_i & \boldsymbol{0} & -\boldsymbol{R}^{-1} \end{bmatrix},$$

$$\hat{\boldsymbol{V}}_{ij} = \begin{bmatrix} \boldsymbol{H}_{ij}+\boldsymbol{H}_{ji} & \boldsymbol{X}\boldsymbol{C}_i^T & -\boldsymbol{M}_j^T & \boldsymbol{X}\boldsymbol{C}_j^T & -\boldsymbol{M}_i^T \\ \boldsymbol{C}_i\boldsymbol{X} & -\boldsymbol{Q}^{-1} & \boldsymbol{0} & \boldsymbol{0} & \boldsymbol{0} \\ -\boldsymbol{M}_j & \boldsymbol{0} & -\boldsymbol{R}^{-1} & \boldsymbol{0} & \boldsymbol{0} \\ \boldsymbol{C}_j\boldsymbol{X} & \boldsymbol{0} & \boldsymbol{0} & -\boldsymbol{Q}^{-1} & \boldsymbol{0} \\ -\boldsymbol{M}_i & \boldsymbol{0} & \boldsymbol{0} & \boldsymbol{0} & -\boldsymbol{R}^{-1} \end{bmatrix},$$

$$\boldsymbol{H}_{ij} = \boldsymbol{X}\boldsymbol{A}_i^T + \boldsymbol{A}_i\boldsymbol{X} - \boldsymbol{B}_i\boldsymbol{M}_j - \boldsymbol{M}_j^T\boldsymbol{B}_i^T.$$

4.2 Simulation Results

The above LMI conditions are feasible. Both SOS design conditions in Theorems 1 and 2 are also feasible. We compare the LMI-based guaranteed-cost controller (designed by solving the (33) - (35)) with the controller (designed by the SOS conditions in Theorem 2), that is, with the SOS-based guaranteed-cost controller. Table 2 shows comparison results of performance function values J for the LMI controller and the SOS controller, where the initial positions are $u(0) = 0.5$, $v(0) = 0.5$, $w(0) = 0.5$ $e_x(0) = -0.6$, $e_y(0) = -0.4$ and $e_z(0) = -1$. In Table 2, Cases I, II and III denote three cases of selecting the weighting matrices $(\boldsymbol{Q}, \boldsymbol{R}) = (\boldsymbol{I}, 0.1\boldsymbol{I})$, $(\boldsymbol{Q}, \boldsymbol{R}) = (\boldsymbol{I}, \boldsymbol{I})$, and $(\boldsymbol{Q}, \boldsymbol{R}) = (\boldsymbol{I}, 10\boldsymbol{I})$, respectively. In the SOS controller design, the order of $\boldsymbol{M}(\boldsymbol{x})$ is one, i.e., all the elements of $\boldsymbol{M}(\boldsymbol{x})$ are permitted to be a linear combination of one order with respect to state variables (namely affine), and the order of $\boldsymbol{X}(\tilde{\boldsymbol{x}})$ is zero, i.e., $\boldsymbol{X}(\tilde{\boldsymbol{x}})$ is a constant matrix.

Table 2. Comparison of performance function values J

	Case I	Case II	Case III
LMI controller	0.57724	1.392	5.0064
SOS controller (Order of M is 1)	0.49951	0.84659	2.8677
Reduction rate of J [%]	13.4658	39.1818	42.7193

It is found from Table 2 that the performance index values of the SOS based guaranteed-cost control (Theorem 2) are better than those of the LMI based guaranteed-cost control ((33) - (35)) in all the cases. When the orders of $\boldsymbol{X}(\tilde{\boldsymbol{x}})$ and $\boldsymbol{M}(\boldsymbol{x})$ are zero, that is, when $\boldsymbol{X}(\tilde{\boldsymbol{x}})$ and $\boldsymbol{M}(\boldsymbol{x})$ are constant matrices instead of polynomial matrices in $\boldsymbol{x}$, the design conditions in Theorems 1 and 2 reduce to the existing LMI design conditions. In other words, when $\boldsymbol{X}(\tilde{\boldsymbol{x}})$ and $\boldsymbol{M}(\boldsymbol{x})$ are constant matrices, the polynomial fuzzy controller reduces to the Takagi-Sugeno fuzzy controller. Thus, the SOS approach provides more relaxed results than the existing LMI approach.

Fig. 1 shows the SOS control result in the following target trajectory: $[x_{ref}\ y_{ref}\ z_{ref}]$ given as [0 0 0] at $t = 0$, [0 0 1] at $0 < t < 60$, [1 0 1] at $60 \leq t < 120$, [1 1 1] at $120 \leq t < 180$, [0 1 1] at $180 \leq t < 240$, and [0 1 0] at $240 \leq t \leq 300$, where $\psi = 0$ for all t. The designed SOS controller perfectly works even for the trajectory task since $\boldsymbol{x}(t) \to 0$ implies $e_x(t) \to 0$, $e_y(t) \to 0$ and $e_z(t) \to 0$. Table 3 shows comparison results of performance function values J in the above trajectory control. The SOS control result is better than the LMI control result also in the trajectory control.

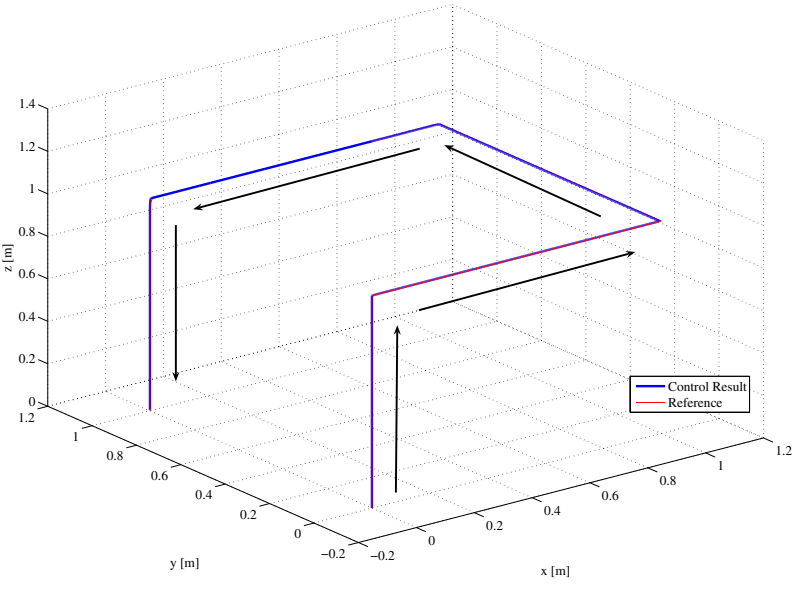

Fig. 1. Trajectory control via SOS control (Case I)

Table 3. Comparison of performance function values J

	Case I	Case II	Case III
LMI controller	0.0479	0.4733	8.0186
SOS controller (Order of M is 1)	0.0274	0.1614	5.1378

5 Vision-Based Micro Helicopter Control in Real Environments

In the previous sections, we have mainly discussed LMI and SOS based fuzzy control system design approaches for the micro helicopter. In this section, we apply one of the approaches to vision-based control of the micro helicopter in real environments [36].

Autonomous control (e.g., [4]-[16]) of helicopters has been conducted for outdoor helicopters with expensive inertial measurement units (IMU) including GPS, 3D acceleration sensors, 3D gyro sensors, etc. On the other hand, it is possible to control a small helicopter with inexpensive (reasonable price) sensors. However, it is, in general, harder to stabilize smaller helicopters due to their smaller moment of inertia in addition to the properties of unstable, nonlinear and coupling.

Fig. 2 shows the micro (palm-size) helicopter that is a co-axial counter rotating helicopter produced by HIROBO. Table 4 shows the specification of helicopter. The weight of the helicopter itself is 200g. It should be noted that the payload is only 60 g due to micro (palm-size) helicopter. Thus, due to the payload restriction, it is difficult to put a 3D acceleration sensor, a 3D gyro sensor and a 3D geomagnetic sensor, etc., on the micro helicopter.

Fig. 2. R/C Micro Helicopter

Table 4. Specification of helicopter

Mass	0.20[kg]	Length	0.40[m]
Width	0.23[m]	Height	0.20 [m]
Blade diameter	0.35 [m]	Payload	60 [g]

We put only a small-light wireless camera on the micro-helicopter. The camera is employed for detecting the position and attitude and for gathering flight visual information. The first point is accomplished by the so-called parallel tracking and mapping (PTAM) [40]. Thus, the PTAM technique using a small single wireless camera on the helicopter is utilized to detect the position and attitude of the helicopter. We construct the measurement system that is able to calibrate the mapping between local coordinate system in the PTAM and world coordinate system and is able to realize noise detection and elimination. In addition, we design the guaranteed cost (stable) controller for the dynamics of the helicopter via an LMI approach. Although path tracking control only via the small single wireless vision sensor is a quite difficult task, the control results demonstrate the utility of our approach. We have verified in the previous sections that the proposed SOS approach is better than the existing LMI approaches. The SOS design for the micro helicopter is currently ongoing and is expected to be presented elsewhere.

Subsection 5.1 presents our experimental system and micro helicopter with a wireless camera. We also discuss the PTAM as a visual SLAM to detect the position and attitude of the helicopter. In addition, we construct the measurement system that is able to calibrate the mapping between local coordinate system in the PTAM and world coordinate system and is able to realize noise detection and elimination. In Subsection 5.2, we design the guaranteed cost (stable) controller for the dynamics of the helicopter via an LMI approach. Subsection 5.3 demonstrates that the constructed system with the guaranteed cost controller achieves path tracking control well even though stabilization of the indoor micro helicopter only via the small single wireless vision sensor is a quite difficult task.

5.1 Experimental System

Fig. 3 shows the experimental system using the small-light wireless camera (TINY-3H) produced by RFSystem Co.,Ltd. The weight is 55 g and is within the payload limitation (60 g). Table 5 summarizes the specification of the wireless camera. The six degree of freedom of the helicopter is calculated by the PTAM based on vision obtained from the wireless camera. After the computation using the PTAM, the control input determined by a stable controller (that will be discussed later) is sent to the helicopter via an R/C transmitter. The sampling rate is 30 [Hz].

In this research, an open-source software, parallel tracking and mapping (PTAM) developed by Klein and Murray [40], is employed to detect the position and attitude of the indoor micro helicopter. The PTAM is a method of estimating camera pose in an unknown scene. They proposed a system specifically designed to track a hand-held camera in a small augmented reality (AR) workspace. For more details of the PTAM, see [40]-[45].

As mentioned before, the PTAM is supposed to use for tracking a hand-held camera in a small AR workspace. Hence, we need to add two functions to achieve stabilization of the micro helicopter.

- Accurate calibration of the mapping between world coordinate system and PTAM coordinate system.
- Compensation of the vision noise contaminated by wireless vision transmission, electromagnetic devices, or body vibrations of the helicopter, etc.

Fig. 4 shows an example of the vision noise contaminated by transmission, electromagnetic devices, or body vibrations of the helicopter, etc., where i-th frame

Table 5. Specification of TINY-3H

Weight	55g
Image Sensor	270000 pixels 1/4 inch color CCD
Unobstructed Effective Range	100m (Transmission distance)
Size	117 18 75

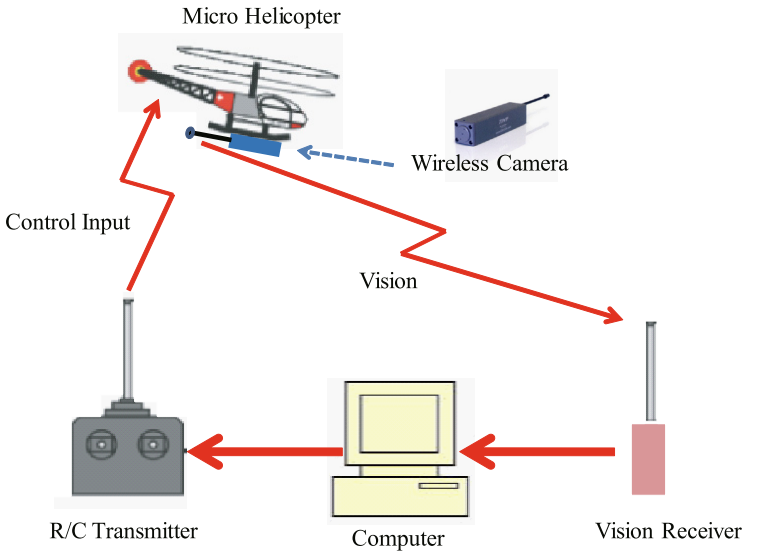

Fig. 3. Experimental System

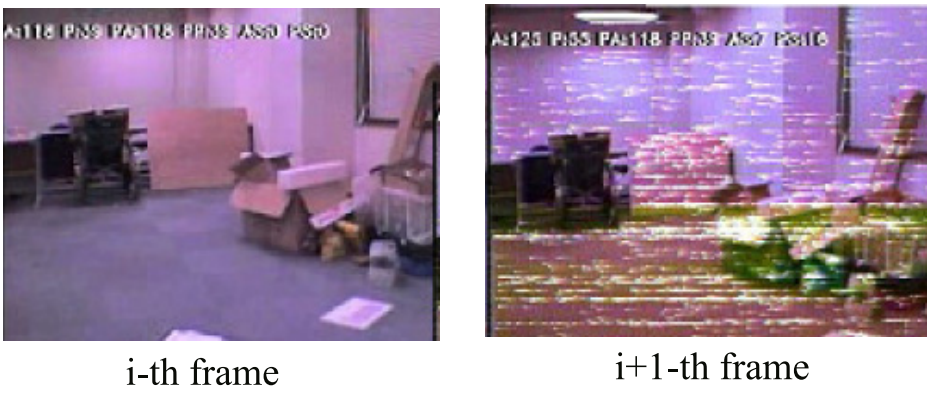

Fig. 4. Vision contaminated by noise

is clear, but i+1-th frame is contaminated by noise. In the i+1-th frame, the position and attitude of the helicopter calculated using the PTAM for noise vision suddenly change for the calculation result from the previous i-th frame. In this case, we ignore the calculation result for the i+1-th frame and still utilizes the calculation result for the previous i-th frame. The threshold of judging the noise frame is ϵ % change of at least one of six variables in the position and attitude. The value of ϵ is adjusted through experiments.

5.2 Controller Design

In this section, we consider also yaw dynamics in addition to (28)-(30). Then, by considering its co-axial counter structure, the restitutive force (generated by a mechanical stabilizer attached on the helicopter) and gravity compensation, the dynamics can be rewritten as

$$\dot{u}(t) = r(t)v(t) + \frac{1}{m}F_X(t), \tag{36}$$

$$\dot{v}(t) = -r(t)u(t) + \frac{1}{m}F_Y(t), \tag{37}$$

$$\dot{w}(t) = \frac{1}{m}F_Z(t), \tag{38}$$

$$\dot{\psi}(t) = \frac{1}{I_Z}U_\psi(t). \tag{39}$$

The approximation is sometimes used in practical control field [46,47] and actually works well. Of course, these papers do not realize wireless vision-based stabilization in addition to without external markers. $U_X(t)$, $U_Y(t)$, $U_Z(t)$ and $U_\psi(t)(\dot{U}_\psi(t) = M_z(t))$ denote new control input variables. We can obtain the original control inputs (to the real helicopter) from $F_X(t)$, $F_Y(t)$, $F_Z(t)$ and $U_\psi(t)$.

By taking time derivative of (36)-(39) and defining the state and control vectors as

$$\boldsymbol{x}(t) = [x(t)\ y(t)\ z(t)\ \psi(t)\ u(t)\ v(t)\ w(t)]^T,$$
$$\boldsymbol{u}(t) = [F_X(t)\ F_Y(t)\ F_Z(t)\ U_\psi(t)]^T,$$

we arrive at the following state equation

$$\frac{d}{dt}\dot{\boldsymbol{x}}(t) = \boldsymbol{A}\dot{\boldsymbol{x}}(t) + \boldsymbol{B}\dot{\boldsymbol{u}}(t) \tag{40}$$

where

$$\boldsymbol{A} = \begin{bmatrix} 0&0&0&0&1&0&0 \\ 0&0&0&0&0&1&0 \\ 0&0&0&0&0&0&1 \\ 0&0&0&0&0&0&0 \\ 0&0&0&0&0&r(t)&0 \\ 0&0&0&0&-r(t)&0&0 \\ 0&0&0&0&0&0&0 \end{bmatrix},$$

$$\boldsymbol{B} = \begin{bmatrix} 0&0&0&0 \\ 0&0&0&0 \\ 0&0&0&0 \\ 0&0&0&\frac{1}{I_Z} \\ \frac{1}{m}&0&0&\frac{1}{I_Z}v(t) \\ 0&\frac{1}{m}&0&-\frac{1}{I_Z}u(t) \\ 0&0&\frac{1}{m}&0 \end{bmatrix},$$

$$\boldsymbol{C} = \begin{bmatrix} 1\,0\,0\,0\,0\,0\,0 \\ 0\,1\,0\,0\,0\,0\,0 \\ 0\,0\,1\,0\,0\,0\,0 \\ 0\,0\,0\,1\,0\,0\,0 \end{bmatrix}.$$

We consider reasonable assumption such that $-u_d \leq u(t) \leq u_d$, $-v_d \leq v(t) \leq v_d$ and $-r_d \leq r(t) \leq r_d$. Applying the sector nonlinearity procedure [28] to the augmented system, we obtain the fuzzy model (41) that exactly represent the dynamics (40) under the assumption. In this case, we set $u_d = 2$, $v_d = 2$ and $r_d = \pi$.

The Takagi-Sugeno fuzzy model for micro helicopter dynamics considering the above two features can be represented as

$$\frac{dt}{d}\dot{\boldsymbol{x}}(t) = \sum_{i=1}^{8} h_i(u(t), v(t), r(t))\{\boldsymbol{A}_i\dot{\boldsymbol{x}}(t) + \boldsymbol{B}_i\dot{\boldsymbol{u}}(t)\}, \tag{41}$$

where

$$\begin{aligned} \boldsymbol{x}(t) &= [x(t)\ y(t)\ z(t)\ \psi(t)\ u(t)\ v(t)\ w(t)]^T, \\ \boldsymbol{u}(t) &= [F_X(t)\ F_Y(t)\ F_Z(t)\ U_\psi(t)]^T, \end{aligned}$$

$$\boldsymbol{A_1} = \boldsymbol{A_3} = \boldsymbol{A_5} = \boldsymbol{A_7} = \begin{bmatrix} 0\,0\,0\,0\,0 & 1 & 0 & 0 \\ 0\,0\,0\,0\,0 & 0 & 1 & 0 \\ 0\,0\,0\,0\,0 & 0 & 0 & 1 \\ 0\,0\,0\,0\,0 & 0 & 0 & 0 \\ 0\,0\,0\,0\,0 & 0 & r_d & 0 \\ 0\,0\,0\,0\,0 & -r_d & 0 & 0 \\ 0\,0\,0\,0\,0 & 0 & 0 & 0 \end{bmatrix},$$

$$\boldsymbol{A_2} = \boldsymbol{A_4} = \boldsymbol{A_6} = \boldsymbol{A_8} = \begin{bmatrix} 0\,0\,0\,0\,0 & 1 & 0 & 0 \\ 0\,0\,0\,0\,0 & 0 & 1 & 0 \\ 0\,0\,0\,0\,0 & 0 & 0 & 1 \\ 0\,0\,0\,0\,0 & 0 & 0 & 0 \\ 0\,0\,0\,0\,0 & 0 & -r_d & 0 \\ 0\,0\,0\,0\,0 & r_d & 0 & 0 \\ 0\,0\,0\,0\,0 & 0 & 0 & 0 \end{bmatrix},$$

$$\boldsymbol{B_1} = \boldsymbol{B_2} = \begin{bmatrix} 0 & 0 & 0 & 0 \\ 0 & 0 & 0 & 0 \\ 0 & 0 & 0 & 0 \\ 0 & 0 & 0 & \frac{1}{I_Z} \\ \frac{1}{m} & 0 & 0 & \frac{v_d}{I_Z} \\ 0 & \frac{1}{m} & 0 & -\frac{u_d}{I_Z} \\ 0 & 0 & \frac{1}{m} & 0 \end{bmatrix}, \boldsymbol{B_3} = \boldsymbol{B_4} = \begin{bmatrix} 0 & 0 & 0 & 0 \\ 0 & 0 & 0 & 0 \\ 0 & 0 & 0 & 0 \\ 0 & 0 & 0 & \frac{1}{I_Z} \\ \frac{1}{m} & 0 & 0 & -\frac{v_d}{I_Z} \\ 0 & \frac{1}{m} & 0 & -\frac{u_d}{I_Z} \\ 0 & 0 & \frac{1}{m} & 0 \end{bmatrix},$$

$$\boldsymbol{B_5} = \boldsymbol{B_6} = \begin{bmatrix} 0 & 0 & 0 & 0 \\ 0 & 0 & 0 & 0 \\ 0 & 0 & 0 & 0 \\ 0 & 0 & 0 & \frac{1}{I_Z} \\ \frac{1}{m} & 0 & 0 & \frac{v_d}{I_Z} \\ 0 & \frac{1}{m} & 0 & \frac{u_d}{I_Z} \\ 0 & 0 & \frac{1}{m} & 0 \end{bmatrix}, \boldsymbol{B_7} = \boldsymbol{B_8} = \begin{bmatrix} 0 & 0 & 0 & 0 \\ 0 & 0 & 0 & 0 \\ 0 & 0 & 0 & 0 \\ 0 & 0 & 0 & \frac{1}{I_Z} \\ \frac{1}{m} & 0 & 0 & -\frac{v_d}{I_Z} \\ 0 & \frac{1}{m} & 0 & \frac{u_d}{I_Z} \\ 0 & 0 & \frac{1}{m} & 0 \end{bmatrix},$$

$$\begin{aligned}
h_1(u(t), v(t), r(t)) =& \frac{u(t) + u_d}{2u_d} \cdot \frac{v(t) + v_d}{2v_d} \cdot \frac{r(t) + r_d}{2r_d}, \\
h_2(u(t), v(t), r(t)) =& \frac{u(t) + u_d}{2u_d} \cdot \frac{v(t) + v_d}{2v_d} \cdot \frac{r_d - r(t)}{2r_d}, \\
h_3(u(t), v(t), r(t)) =& \frac{u(t) + u_d}{2u_d} \cdot \frac{v_d - v(t)}{2v_d} \cdot \frac{r(t) + r_d}{2r_d}, \\
h_4(u(t), v(t), r(t)) =& \frac{u(t) + u_d}{2u_d} \cdot \frac{v_d - v(t)}{2v_d} \cdot \frac{r_d - r(t)}{2r_d}, \\
h_5(u(t), v(t), r(t)) =& \frac{u_d - u(t)}{2u_d} \cdot \frac{v(t) + v_d}{2v_d} \cdot \frac{r(t) + r_d}{2r_d}, \\
h_6(u(t), v(t), r(t)) =& \frac{u_d - u(t)}{2u_d} \cdot \frac{v(t) + v_d}{2v_d} \cdot \frac{r_d - r(t)}{2r_d},
\end{aligned}$$

$$\begin{aligned}
h_7(u(t), v(t), r(t)) =& \frac{u_d - u(t)}{2u_d} \cdot \frac{v_d - v(t)}{2v_d} \cdot \frac{r(t) + r_d}{2r_d}, \\
h_8(u(t), v(t), r(t)) =& \frac{u_d - u(t)}{2u_d} \cdot \frac{v_d - v(t)}{2v_d} \cdot \frac{r_d - r(t)}{2r_d}.
\end{aligned}$$

By defining the error $\boldsymbol{e}(t) = \boldsymbol{r} - \boldsymbol{y}(t)$, we have the following augmented system.

$$\frac{d}{dt}\hat{\boldsymbol{x}}(t) = \sum_{i=1}^{8} h_i(u(t), v(t), r(t))\{\hat{\boldsymbol{A}}_i\hat{\boldsymbol{x}}(t) + \hat{\boldsymbol{B}}_i\hat{\boldsymbol{u}}(t)\} \tag{42}$$

$$\boldsymbol{y}(t) = \sum_{i=1}^{8} h_i(u(t), v(t), r(t))\hat{\boldsymbol{C}}_i\hat{\boldsymbol{x}}(t), \tag{43}$$

where $\hat{\boldsymbol{u}}(t) = \dot{\boldsymbol{u}}(t)$,

$$\hat{\boldsymbol{x}}(t) = \begin{bmatrix} \dot{\boldsymbol{x}}(t) \\ \boldsymbol{e}(t) \end{bmatrix}, \ \hat{\boldsymbol{A}}_i = \begin{bmatrix} \boldsymbol{A}_i & 0 \\ \hat{\boldsymbol{C}}_i & 0 \end{bmatrix}, \ \hat{\boldsymbol{B}}_i = \begin{bmatrix} \boldsymbol{B}_i \\ 0 \end{bmatrix},$$

$$\hat{\boldsymbol{C}}_i = \begin{bmatrix} 1 & 0 & 0 & 0 & 0 & 0 & 0 \\ 0 & 1 & 0 & 0 & 0 & 0 & 0 \\ 0 & 0 & 1 & 0 & 0 & 0 & 0 \\ 0 & 0 & 0 & 1 & 0 & 0 & 0 \end{bmatrix}.$$

We design the following dynamic fuzzy controller to stabilize the augmented system.

$$\hat{\boldsymbol{u}}(t) = -\sum_{i=1}^{8} h_i(u(t), v(t), r(t))\boldsymbol{F}_i\hat{\boldsymbol{x}}(t) \tag{44}$$

Let us consider the following performance function to be optimized.

$$J = \int_0^\infty \hat{\boldsymbol{y}}^T(t) \begin{bmatrix} \boldsymbol{Q} & \boldsymbol{0} \\ \boldsymbol{0} & \boldsymbol{R} \end{bmatrix} \hat{\boldsymbol{y}}(t)dt, \tag{45}$$

where

$$\hat{\boldsymbol{y}}(t) = \begin{bmatrix} \boldsymbol{y}(t) \\ \hat{\boldsymbol{u}}(t) \end{bmatrix} = \sum_{i=1}^{r}\sum_{j=1}^{r} \hat{h}_i(t)\hat{h}_j(t) \begin{bmatrix} \hat{\boldsymbol{C}}_i \\ -\boldsymbol{F}_j \end{bmatrix} \hat{\boldsymbol{x}}(t), \tag{46}$$

$\boldsymbol{Q}$ and $\boldsymbol{R}$ are positive definite matrices, and $\hat{h}_i(t) = h_i(u(t), v(t), r(t))$.

We can find feedback gains that minimizes the upper bound of (45) by solving the following linear matrix inequalities (LMIs) (47)-(49) [28]. From the solutions $\boldsymbol{X}$ and $\boldsymbol{M_i}$, the feedback gains can be obtained as $\boldsymbol{F}_i = \boldsymbol{M}_i\boldsymbol{X}^{-1}$. Then, the controller satisfies $J < \boldsymbol{x}^T(0)\boldsymbol{X}\boldsymbol{x}(0) < \lambda$.

$$\begin{aligned} &\underset{\boldsymbol{X},\boldsymbol{M_i},}{minimize}\ \lambda \\ &subject\ to \end{aligned}$$

$$\boldsymbol{X} > \boldsymbol{0},\ \begin{bmatrix} \lambda & \boldsymbol{x}^T(0) \\ \boldsymbol{x}(0) & \boldsymbol{X} \end{bmatrix} > \boldsymbol{0}, \tag{47}$$

$$\hat{\boldsymbol{U}}_{ii} < \boldsymbol{0} \tag{48}$$

$$\hat{\boldsymbol{V}}_{ij} < \boldsymbol{0} \qquad i < j, \tag{49}$$

where

$$\hat{\boldsymbol{U}}_{ii} = \begin{bmatrix} \boldsymbol{H}_{ii} & \boldsymbol{X}\hat{\boldsymbol{C}}_i^T & -\boldsymbol{M}_i^T \\ \hat{\boldsymbol{C}}_i\boldsymbol{X} & -\boldsymbol{Q}^{-1} & \boldsymbol{0} \\ -\boldsymbol{M}_i & \boldsymbol{0} & -\boldsymbol{R}^{-1} \end{bmatrix},$$

$$\hat{\boldsymbol{V}}_{ij} = \begin{bmatrix} \boldsymbol{H}_{ij} + \boldsymbol{H}_{ji} & \boldsymbol{X}\hat{\boldsymbol{C}}_i^T & -\boldsymbol{M}_j^T & \boldsymbol{X}\hat{\boldsymbol{C}}_j^T & -\boldsymbol{M}_i^T \\ \hat{\boldsymbol{C}}_i\boldsymbol{X} & -\boldsymbol{Q}^{-1} & \boldsymbol{0} & \boldsymbol{0} & \boldsymbol{0} \\ -\boldsymbol{M}_j & \boldsymbol{0} & -\boldsymbol{R}^{-1} & \boldsymbol{0} & \boldsymbol{0} \\ \hat{\boldsymbol{C}}_j\boldsymbol{X} & \boldsymbol{0} & \boldsymbol{0} & -\boldsymbol{Q}^{-1} & \boldsymbol{0} \\ -\boldsymbol{M}_i & \boldsymbol{0} & \boldsymbol{0} & \boldsymbol{0} & -\boldsymbol{R}^{-1} \end{bmatrix},$$

$$\boldsymbol{H}_{ij} = \boldsymbol{X}\boldsymbol{A}_i^T + \boldsymbol{A}_i\boldsymbol{X} - \boldsymbol{B}_i\boldsymbol{M}_j - \boldsymbol{M}_j^T\boldsymbol{B}_i^T.$$

It should be noted that the controller satisfying the LMIs (47)-(49) is a stable controller.

5.3 Experimental Results

Control experiment is performed from the take-off on the floor at the origin $(x(0), y(0), z(0)) = (0[mm], 0[mm], 0[mm])$ and rectangular trajectory flight during keeping z(t)=1000 [mm]. The vertex points of the rectangular trajectory are Point A (0 [mm], 0 [mm], 1000 [mm]), Point B (2000 [mm], 0 [mm], 1000 [mm]), Point C (2000 [mm], 1500 [mm], 1000 [mm]) and Point D (0 [mm], 1500 [mm], 1000 [mm]). The flight task is to make two circles around Points A, B, C and D during keeping the altitude z(t)=1000 [mm].

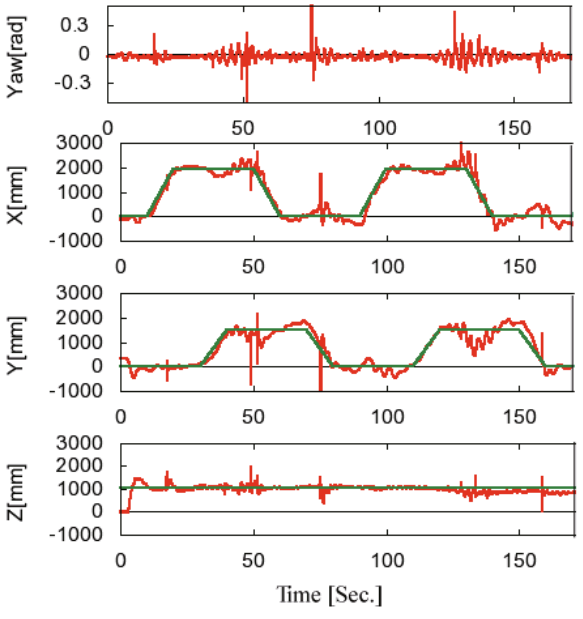

Fig. 5. Experimental result of path tracking flight

Fig. 5 shows the trajectory control result (yaw, x, y and z) via the fuzzy controller, where the target (green lines) and control result (red lines) are plotted. It can be seen that the helicopter can follow the trajectory well even though the impulse noises are sometimes caused by wireless vision transmission, electromagnetic devices, or body vibrations of the helicopter, etc. Thus, the control result shows the utility of our wireless vision-based control system. Fig 6 shows photographs of the experimental result, where the red boxes indicate the positions of the micro helicopter and the small window in each the photograph shows vision views from the wireless camera on the micro helicopter. It should be noted that the trajectory of the micro helicopter is stabilized only by using the wireless vision sensor without 3D acceleration sensors, 3D gyro sensors and 3D geomagnetic sensors, etc., in addition to without external markers.

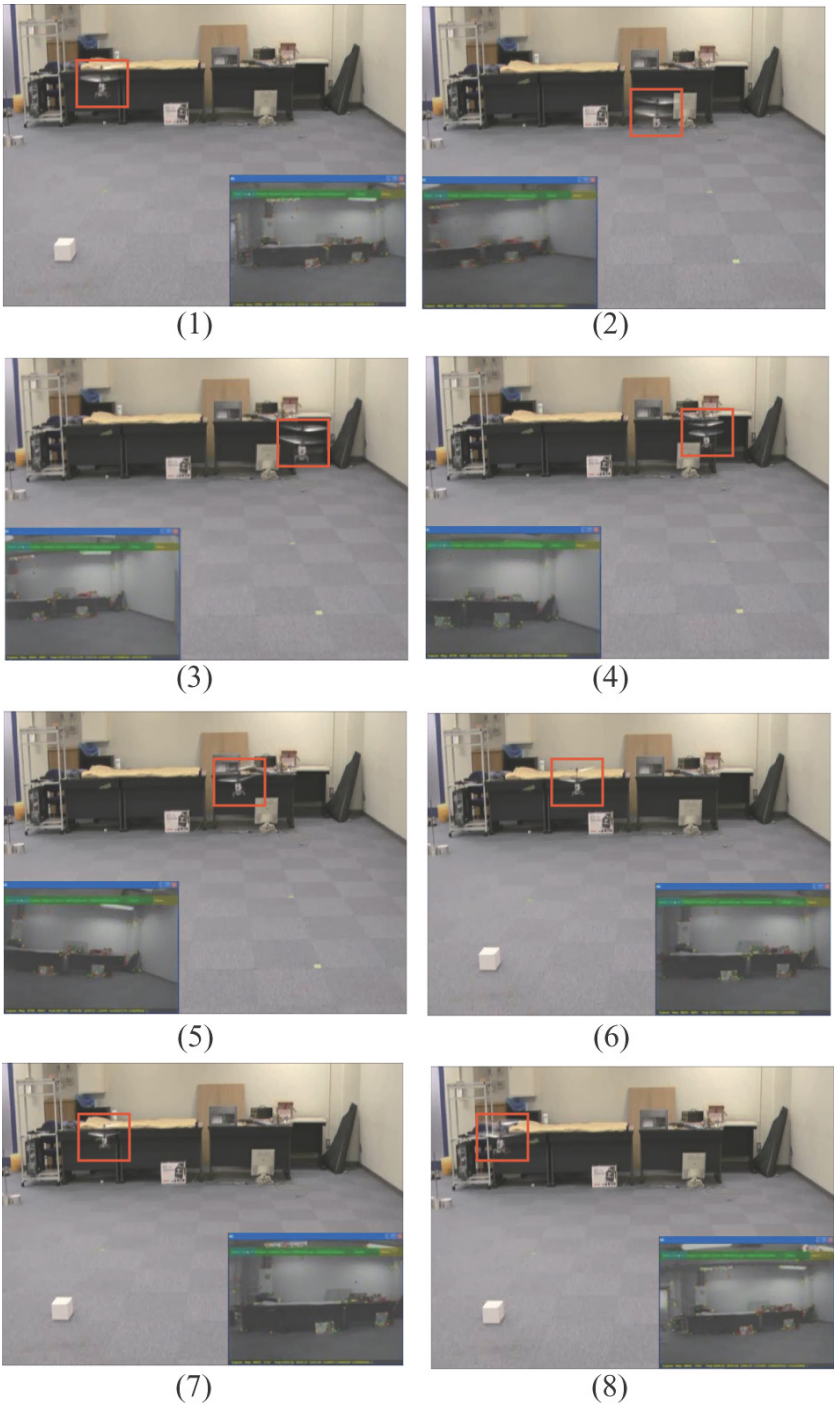

Fig. 6. Experimental results (photos)

6 Conclusions

The former of this chapter has presented a comparison result of micro helicopter control via a typical linear matrix inequality (LMI) approach and a sum of squares (SOS) approach. The SOS design approach discussed in this chapter is more general than that based on the existing LMI design approaches to T-S fuzzy control systems. The control results of a micro helicopter have shown that the SOS design approach provides better control results than the LMI design approach.

The latter of this chapter has presented wireless vision-based stabilization of an indoor micro helicopter via visual simultaneous localization and mapping (SLAM). The PTAM technique using a small single wireless camera on the helicopter has been utilized to detect the position and attitude of the helicopter. We have also constructed the measurement system that is able to calibrate the mapping between local coordinate system in the PTAM and world coordinate system and is able to realize noise detection and elimination. In addition, we have designed the guaranteed cost (stable) controller for the dynamics of the helicopter via a linear matrix inequality (LMI) approach. The path tracking control results only via the small single wireless vision sensor have demonstrated the utility of our approach.

Our next target is to realize vision-based formation control of plural micro helicopters.

References

1. http://www.rc.mce.uec.ac.jp/
2. http://www.bu.edu/me/people/faculty/pz/wang/
3. Nonami, K.: Rotating Wing Aerial Robotics. Journal of the Robotics Society of Japan 24(8), 890–896 (2006)
4. Sugeno, M., et al.: Intelligent Control of an Unmanned Helicopter Based on Fuzzy Logic. In: Proc. of American Helicopter Society 51st Annual Forum, Texas (May 1995)
5. Sugeno, M.: Development of an Intelligent Unmanned Helicopter. In: Nguyen, H.T., Prasad, N.R. (eds.) Fuzzy Modeling and Control: Selected Works of M. Sugeno. CRC Press (1999)
6. Ohtake, H., Iimura, K., Tanaka, K.: Fuzzy Control of Micro Helicopter with Coaxial Counter-rotating Blades. In: SCIS and ISIS 2006, Tokyo, pp. 1955–1958 (September 2006)
7. Yoshihata, Y., Watanabe, K., Iwatani, Y., Hashimoto, K.: Multi-camera visual servoing of a micro helicopter under occlusions. In: 2007 IEEE/RSJ International Conference on Intelligent Robots and Systems, San Diego, CA, USA, pp. 2615–2620 (October 2007)
8. Wang, W., et al.: Autonomous Control for Micro-Flying Robot and Small Wireless Helicopter X.R.B. In: 2006 IEEE/RSJ International Conference on Intelligent Robots and Systems, Beijing, pp. 2906–2911 (October 2006)
9. Mori, R., Kubo, T., Kinoshita, T.: Vision-Based Hovering Control of a Small-Scale Unmanned Helicopter. In: SICE-ICASE International Joint Conference 2006, pp. 1274–1278 (2006)

10. Pastor, E., Lopez, J., Royo, P.: UAV Payload and Mission Control Hardware/Software Architecture. IEEE Aerospace and Electronic Systems Magazine 22(6), 3–8 (2007)
11. Antsev, G.V., et al.: UAV landing system simulation model software system. IEEE Aerospace and Electronic Systems Magazine 26(3), 26–29 (2011)
12. Lin, Y., Hyyppa, J., Jaakkola, A.: Mini-UAV-Borne LIDAR for Fine-Scale Mapping. IEEE Geoscience and Remote Sensing Letters 8(3), 426–430 (2011)
13. Kumon, M., et al.: Autopilot System for Kiteplane. IEEE/ASME Transactions on Mechatronics 11(5), 615–624 (2006)
14. Tanaka, K., et al.: Development of a Cyclogyro-Based Flying Robot With Variable Attack Angle Mechanisms. IEEE/ASME Transactions on Mechatronics 12(5), 565–570 (2007)
15. Jinok, S., et al.: Attitude Control and Hovering Control of Radio-Controlled Helicopter. Journal of the JSME, Part C 68(675), 3284–3291 (2002)
16. Kanade, T., Amidi, O., Ke, Q.: Real-time and 3D vision for autonomous small and micro air vehicles. In: 43rd IEEE Conference on Decision and Control, pp. 1655–1662 (2004)
17. Wu, H., Sun, D., Zhou, Z.: Micro air vehicle: configuration, analysis, fabrication, and test. IEEE/ASME Transactions on Mechatronics 9(1), 108–117 (2004)
18. Madangopal, R., Khan, Z.A., Agrawal, S.K.: Energetics-based design of small flapping-wing micro air vehicles. IEEE/ASME Transactions on Mechatronics 11(4), 433–438 (2006)
19. Gebre-Egziabher, D., Elkaim, G.H.: MAV attitude determination by vector matching. IEEE Transactions on Aerospace and Electronic Systems 44(3), 1012–1028 (2008)
20. McIntosh, S.H., et al.: Design of a mechanism for biaxial rotation of a wing for a hovering vehicle. IEEE/ASME Transactions on Mechatronics 11(2), 145–153 (2006)
21. Valenti, M., Bethke, B., How, J.P., de Farias, D.P., Vian, J.: Embedding Health Management into Mission Tasking for UAV Teams. In: Proceedings of American Control Conference 2007, pp. 5777–5783 (2007)
22. Ohtake, H., et al.: Fuzzy Control of Micro RC Helicopter with Coaxial Counter-rotating Blades. Journal of Society for Fuzzy Theory and Intelligent Informatics 21(1), 100–106 (2009)
23. Wang, W., et al.: Autonomous Control for Micro-Flying Robot and Small Wireless Helicopter X.R.B. In: 2006 IEEE/RSJ International Conference on Intelligent Robots and Systems, Beijing, pp. 2906–2911 (October 2006)
24. Mori, R., Kubo, T., Kinoshita, T.: Vision-Based Hovering Control of a Small-Scale Unmanned Helicopter. In: SICE-ICASE International Joint Conference 2006, pp. 1274–1278 (2006)
25. Hirose, H., et al.: Visual Feedback Control of a Small RC Helicopter Using a Vehicle-Mounted Camera. In: 49th Administration Committee of Japan Joint Automatic Control Conference, pp. 332–335 (2006)
26. Mori, R., et al.: Vision-Based Guidance Control of a Small-Scale Unmanned Helicopter. In: Proceedings of the 2007 IEEE/RSJ International Conference on Intelligent Robots and Systems, pp. 2648–2653 (2007)
27. Iimura, K., et al.: Position Estimation and Control of an Indoor Micro Helicopter using an Attached Single Camera. In: The Proceedings of RoboMec Symposium 2009, Fukuoka, pp. 215–218 (May 2009)
28. Tanaka, K., Wang, H.O.: Fuzzy Control Systems Analysis and Design: A Linear Matrix Inequality Approach. John Wiley and Sons Publisher, New York (2001)

29. Tanaka, K., Yoshida, H., Ohtake, H., Wang, H.O.: A Sum of Squares Approach to Stability Analysis of Polynomial Fuzzy Systems. In: 2007 American Control Conference, New York, pp. 4071–4076 (July 2007)
30. Tanaka, K., Ohtake, H., Wang, H.O.: A Sum of Squares Approach to Modeling and Control of Nonlinear Dynamical Systems with Polynomial Fuzzy Systems. IEEE Transactions on Fuzzy Systems 17(4), 911–922 (2009)
31. Tanaka, K., Ohtake, H., Wang, H.O.: An SOS-based Stable Control of Polynomial Discrete Fuzzy Systems. In: 2008 American Control Conference, Seattle, Washington, pp. 4881–4886 (June 2008)
32. Tanaka, K., Ohtake, H., Wang, H.O.: Guaranteed Cost Control of Polynomial Fuzzy Systems via a Sum of Squares Approach. IEEE Transactions on Systems, Man and Cybernetics Part B 39(2), 561–567 (2009)
33. Tanaka, K., Ohtake, H., Wang, H.O.: A Sum of Squares Approach to Guaranteed Cost Control of Polynomial Discrete Fuzzy Systems. In: 17th IFAC World Congress, Seoul, Korea, pp. 6850–6854 (July 2008)
34. Prajna, S., Papachristodoulou, A., Seiler, P., Parrilo, P.A.: SOSTOOLS:Sum of Squares Optimization Toolbox for MATLAB, Version 2.00 (2004)
35. Sturm, J.F.: Using SeDuMi 1.02:a MATLAB toolbox for optimization over symmetric cones. Optimization Methods and Software 11(1), 625–653 (1999)
36. Tanaka, K., Ohtake, H., Tanaka, M., Wang, H.O.: Wireless Vision-based Stabilization of Indoor Micro Helicopter. IEEE/ASME Transactions on Mechatronics (accepted)
37. Takagi, T., Sugeno, M.: Fuzzy Identification of Systems and Its Applications to Modeling and Control. IEEE Trans. on SMC 15(1), 116–132 (1985)
38. Parrilo, P.A.: Structured Semidefinite Programs and Semialgebraic Geometly Methods in Robustness and Optimization. PhD thesis, California Institute of Technology, Pasadena, CA (2000)
39. Feng, G.: A Survey on Analysis and Design of Model-Based Fuzzy Control Systems. IEEE Trans. on Fuzzy Systems 14(5), 676–697 (2006)
40. Klein, G., Murray, D.: Parallel Tracking and Mapping for Small AR Workspaces. In: Proc. International Symposium on Mixed and Augmented Reality (ISMAR 2007), Nara (2007)
41. Davison, A., Reid, I., Molton, N.D., Stasse, O.: MonoSLAM: Realtime single camera SLAM. IEEE Trans. Pattern Analysis and Machine Intelligence 29(6), 1052–1067 (2007)
42. Eade, E., Drummond, T.: Edge landmarks in monocular slam. In: Proc. British Machine Vision Conference (BMVC 2006), Edinburgh (September 2006); BMVA
43. Eade, E., Drummond, T.: Scalable monocular slam. In: Proc. IEEE Intl. Conference on Computer Vision and Pattern Recognition (CVPR 2006), New York, NY, pp. 469–476 (2006)
44. Smith, R.C., et al.: On the representation and estimation of spatial uncertainty. International Journal of Robotics Research 5(4), 56–68 (1986)
45. Stewénius, H., Engels, C., Nistér, D.: Recent developments on direct relative orientation. ISPRS Journal of Photogrammetry and Remote Sensing 60, 284–294 (2006)
46. Komatsu, T., et al.: Model-based Control of a Small Indoor-type Helicopter. In: The Proceedings of RoboMec Symposium 2008, Nagano, pp. 101–104 (May 2008)
47. Tanaka, K., et al.: Micro Helicopter Control. In: IEEE World Congress on Computational Intelligence, Hong Kong, pp. 347–353 (June 2008)